Strojniški vestnik - Journal of Mechanical Engineering 69(2023)3-4, 87-99
© 2023 The Authors. CC BY 4.0 Int. Licensee: SV-JME
DOI:10.5545/sv-jme.2022.455
Original Scientific Paper
Received for review: 2022-11-18
Received revised form: 2023-01-23
Accepted for publication: 2023-03-06

Effects of Single/Compound Pit Texture on the Friction-induced Vibration and Noise of Thrust Cylindrical Roller Bearings

Yueyong Wang[1,2] – Yimin Zhang[1,2,*] – Yibing Wang[1,2] – Risheng Long[1]
[1]Shenyang University of Chemical Technology, Equipment Reliability Institute, China
[2]Shenyang University of Technology, School of Mechanical Engineering, China

To improve the reliability and service life of thrust cylindrical roller bearings (TCRBs), the effects of single/compound pit texture on tribological properties and on friction-induced vibration and noise were studied. Laser marking equipment was used to create compound pit texture on a shaft washer. A universal friction and wear test rig was used to measure the friction force, vibration acceleration, and noise signals of TCRBs. The differences between the single/composite pit-textured and non-textured surfaces were studied in terms of the friction, wear, and vibration noise properties. The results revealed that the friction force and wear loss of the single/composite pit-textured surface were markedly lower than those of the non-textured surface. Compared to non-textured surface bearings, the friction force and wear loss for textured surface bearings were reduced by 39.6 % and 59.6 %, respectively, when the diameter, depth, and area density of the pit were 300 *μm*, 10 *μm*, and 10 %, respectively. The single/composite pit-textured surface exhibited good potential for vibration absorption and noise suppression. It could effectively interfere with the self-excited vibration of the TCRBs friction pair system, thereby reducing the degree of vibration noise of the TCRBs.
Keywords: thrust cylindrical roller bearings, single/compound pit texture, friction force, wear, friction-induced vibration and noise

Highlights
- *A single/compound surface pitting texture was applied to thrust cylindrical roller bearings under starved conditions.*
- *The friction and wear of single/compound pitted textured cylindrical roller bearings were significantly lower than those of non-textured surface bearings.*
- *Compound pitted textured contact surfaces with regular geometry were more likely to trap worn debris in the pits.*
- *Friction was closely related to vibration and noise, and both single and compound pits contributed to the vibration absorption and noise reduction.*

0 INTRODUCTION

In mechanical systems, thrust cylindrical roller bearings (TCRBs) are commonly used to bear friction losses, axial loads, and to support parts **[1]**. Bearings installed in heavy machines sometimes operate under mixed or starved lubrication; therefore, they show increased friction and wear **[2]**. Friction is caused when two solid surfaces in contact move (or tend to move) relative to each other; Wear is the phenomenon of continuous loss of surface materials in the process of relative movement of pairs, and wear is the inevitable result of friction. Friction causes energy consumption, wear leads to material loss, large material loss will lead to the failure of mechanical parts. Surface wear is a complex process. In an era of expanding energy demand and decreasing non-renewable resources, friction and wear will significantly increase fuel consumption, reduce the energy utilisation rate, and shorten the life of mechanical parts. To reduce these, it is essential to improve the wear resistance of TCRBs. New strategies for modifying friction and wear problems are more urgent now than in any previous era **[3]**. Wear is the inevitable result of friction, it is accompanied by friction process, can only be minimized but not completely avoided. With the development of science and technology, domestic and foreign scholars have found that the friction and wear cannot be greatly reduced if the roughness of the material surface is reduced, but the texture of the surface has better tribological properties. Surface texture has outstanding effects in reducing friction, reducing wear, and improving lubrication properties, which has attracted worldwide attention. Nature presents numerous multi-scale cases, such as the self-cleaning and superhydrophobicity of lotus leaves, adjustable adhesion of gecko feet, and drag reduction on dolphins and shark skin. These natural phenomena suggest that the compound surface pattern can effectively reduce friction and wear.

The lubrication condition of the working surface can be significantly improved by preparing micropits or microgrooves with specific geometries on the contact surface of the friction pair. The tribological properties of such contact surface were also significantly improved **[4]** and **[5]**. Laser surface texture (LST) **[6]**, and **[7]** is one of the most successful methods owing to its flexibility, environmental protection, and economic advantages. Marian et al. **[8]** and **[9]** obtained an optimised and robust micro-texture design through friction simulation combined with advanced data analysis methods and corresponding

*Corr. Author's Address: Shenyang University of Chemical Technology, Equipment Reliability Institute, China, zhangyimin@syuct.edu.cn

tests. Costa et al. [10] emphasised the mechanism causing an increase in friction, pointing out existing deficiencies and future research directions. König et al. [11] numerically predicted the friction performance of journal bearings in single- and multi-scale surface patterns. They found that compared with unpatterned shaft sleeve, the wear of multi-scale patterns was reduced by 80 % at most. The single-scale features of the microcoined and laser patterns reduced the wear by 78 % and 65 %, respectively. Grützmacher et al. [12] experimentally studied the influence of single- and multi-scale surface patterns on the friction properties of sliding bearings, and the coefficients of friction (COFs) of all patterns were significantly reduced. Other encouraging numerical and experimental results showed that multi-scale or hierarchical patterns/textures were significantly improved compared to single pitted and non-textured surfaces [13] to [16]. Milčić et al. [17] studied the effects of shaft bush rotation frequency and radial load on Tegotenax V840 Stann-Babbabt bearings under hydrodynamic lubrication. Wrzochal et al. [18] introduced the basic assumption and mechanical design of a new type of friction torque measuring device for rolling bearings, and made a preliminary evaluation of its indexes.

Numerous studies have shown that friction-induced vibration noise was affected by factors such as the normal load, contact surface properties, and environmental conditions, particularly the microscopic morphology of the contact surface. Sudeep et al. [19], and [20] studied the influence of texture surfaces on friction wear and friction-induced vibration behaviour in the linear reciprocating motion of bearing steel point contact under different working conditions. For certain textures, the vibration amplitude was significantly reduced owing to the increase in the damping value compared to that of the smooth surface. Under starved and full lubrication conditions, Gupta et al. [21] conducted tribological and vibration studies on textured spur pairs. The results showed that the vibration amplitude, temperature rise, and mating surface wear decreased in the presence of a surface texture. Hu et al. [22] studied friction-screaming noise suppression using grooves and round-pit textures. The results indicated that both textured surfaces could reduce the high-frequency screaming noise of the friction system. Wrzochal et al. [23] pointed out that the cleanliness of bearings is a key factor to determine whether rolling bearings meet the quality requirements. Chernets et al. [24] proposed a computational method to solve the plane contact problem of elastic theory to determine the contact strength and tribological durability of plain bearings. Kydyrbekuly et al. [25] proposed a method for amplitude calculation and frequency characteristic construction of forced vibration and self-excited vibration of rotor-fluid-foundation system of nonlinear rolling bearing based on complex amplitude and harmonic balance method.

The relationship between the surface texture of rolling bearings and frictional vibration and noise, particularly for the surface compound texture, is insufficient. The novelty of this work lies in that there is little research on the relationship between surface texture and frictional vibration and noise, especially the relationship between tribological behavior of surface texture rolling bearings and frictional vibration and noise characteristics has not been reported. The research of this content can further study the generation mechanism of friction noise and put forward the optimized surface texture specification to reduce friction noise. An in-depth study and analysis of the mechanism of frictional vibration noise and interface behaviour characteristics of surface compound texture enriches the theory of friction-induced vibration and noise and has essential engineering application value.

1 EXPERIMENT

The TCRB had 18 roller elements (Detailed performance parameters are shown in Table 1), as shown in Fig. 1a. Seven bearing sets labelled G01 to G07 (Table 2), were used to study the effects of single/compound pits on the tribological properties and friction-induced vibration noise of TCRBs. Non-textured TCRBs were introduced as a reference group and coded as G08. Each group contained three TCRBs. The friction force curve for each group was the mean. The wear loss for each group was the average of nine measurements from 24 TCRBs. All TCRBs were the same batch product from the same manufacturer, and

Table 1. *Detailed performance parameters of 81107TN thrust cylindrical roller bearing*

Material	Hardness	Density [g/cm^3]	Elasticity modulus [MPa]	Poisson's ratio	Melting point [°C]	Pyroconductivity [W/(mK)]	Distortion temperature [°C]
GCr15	60 HRC to 65 HRC	7.81	2.07E5	0.29	1395 to 1403	40.11	—
PA66	95 HK to 105 HK	1.24	2.6E3	0.35	250 to 260	—	70

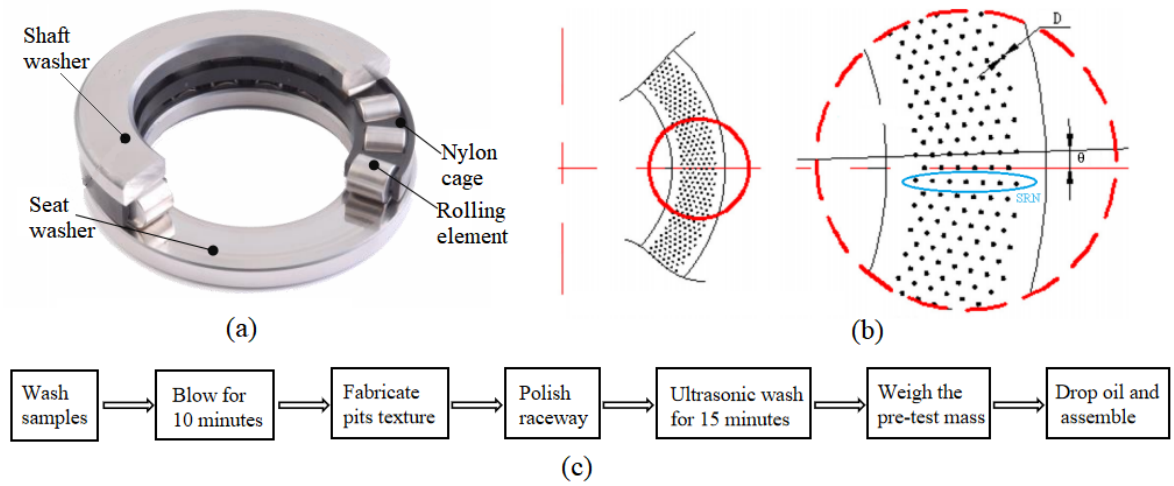

Fig. 1. *a) Components of 81107TN, b) pits texture parameters, and c) treatment process of bearings before wear tests*

the same sample was weighed three times to take the average value.

All TCRBs were prepared before the friction and wear tests according to the process shown in Fig. 1c. Laser marking equipment was used to fabricate compound pit texture on the shaft washer (WS). The textured surface was the surface in contact with the cylindrical roller. After laser texturing, use 800#, 1500#, 2000# sand-papers successively to remove the micro-bulges along the edges of pits by hand. Under the same conditions, the same person grinding with the same force, manual grinding was only the slightly convex edge produced by the pit texture, which did not reach the overall running in state of the bearing.

To reflect the ability of single/compound pits to collect and store debris [26], the effective volume of pits (EVP) was introduced and defined as:

Table 2. *Pits texture parameters and patterns of 81107TN TCRB groups*

Group Code	Diameter, D [μm]	Depth, H [μm]	Density, S [%]	Circumferential angle of pits, θ [°]	Single radial number, SRN	Effective volume of pits, EVP	Pit patterns
G01	100	10	10	1	35	9.891	
G02	300	10	10	1.8	7	9.891	
G03	500	10	10	5	7	9.891	
G04	100 / 300	10	10	2 / 2	35 / 5	11.304	
G05	100 / 500	10	10	2 / 6	35 / 5	10.833	
G06	100 / 100+300	10 / 20	18	1 / 2	35 / 7	17.804	
G07	100 / 100+500	10 / 20	13	1 / 5	35 / 7	18.793	
G08	—	—	—	—	—	—	

$$EVP = \pi \times \left(\frac{D}{2}\right)^2 \times H \times \frac{360^\circ}{\theta} \times SRN \times 10^{-8}. \quad (1)$$

The definition of the terms in Eq. (1) and the calculation results are shown in Fig. 1b and Table 1.

The laser texture parameters are listed in Table 3. The laser pulse duration, also known as Pulse-width, is a unit of time measurement, referring to the duration of laser action. In this study, pulse width ≤5 ms. The pit texture parameters are shown in Fig. 1b. The preparation of different parameters and patterns of the pits on the G01 to G07 shaft washers is shown in Table 1.

Table 3. *Parameters of laser marking equipment*

Indicators category	Parameter
Power [W]	3
Wavelength [nm]	1060
Engraving depth [mm]	0.01
Linear velocity [mm/s]	100
Laser frequency [kHz]	60
Repeated precision [mm]	±0.002

Frictional wear and vibration noise tests of the single/compound pit texture TCRBs were performed using a universal friction and wear test rig (MMW-1A, China) and a multifunctional vibration and noise acquisition system. The test apparatus was composed of friction and wear test system, signal acquisition, analysis system, etc., which could synchronously collect friction and vibration and noise signals in the process of friction and wear test.

The parameters of the universal friction and wear test rig were: longitudinal loading force (2600±100 N), rotational speed (250 rpm), and test time (11000 s). Usually, the rolling bearing is calculated according to the million speed or working hours, and the rotation speed calculated according to the number of revolutions of 250 rpm is 0.6 m/s. Within the test period, the middle distance of operation was 6600 m. Taking into account the effect of sliding ratio, the sliding distance of G02 was 422.4 m and that of G08 was 607.2 m. Before each test, the shaft washer of the bearing was first weighed using an electronic balance (accuracy and readability of 0.1 mg and 0.01 mg, respectively). Drip 10 mg of commercial lubricant (Parameters are shown in Table 4) was applied on the pit-textured surface. All the friction, wear, vibration, and noise tests strictly implemented the above operating steps to ensure consistency in all the bearing tests. Lubricating oil was not used during the test.

Table 4. *Parameters of commercial lubricant*

Indicators category	Unit	Parameter
Dynamic viscosity @ 30 °C	mm²/s	14.45
Density @ 30 °C	kg/l	0.8678
Viscosity index, VI		163
Low temperature pumping viscosity, MRV @ –35 °C	mPa·s	18000
Flash point	°C	242
Pour point	°C	–45

The parameters of the triaxial piezoelectric acceleration sensor and microphone are presented in Table 5. The microphone was placed 30 mm from the friction pair. Vibration and noise signals were acquired using a 16-channel signalling system three times at 1 h intervals, with a sampling frequency and time of 12.8 kHz and 10 s, respectively.

Table 5. *Parameters of triaxial piezoelectric acceleration sensor and microphone*

Parameter	Triaxial piezoelectric acceleration sensor	Microphone
Range	±50 g	17 dB to138 dB
Frequency	0.5 kHz to7 kHz	3.15 Hz to 20 kHz
Sensitivity	10 mV/(m·s²)	50 mV/Pa
Mass	15 g	—

Three groups of bearings with the same texture style were tested under the same working conditions, and the test data (friction force, vibration acceleration, noise, etc.) were the average values of the three tests. All tests were performed under atmospheric conditions of 30±10 % relative humidity and room temperature of approximately 20 °C. The TCRB was cleaned after the tests using an ultrasonic cleaning machine containing an acetone solution. The bearing shaft washer was weighed using an electronic balance. The wear surface of the shaft washer was characterised using a scanning electron microscope. The relationship between the vibration and noise properties of the sample and its tribological behaviour were considered.

2 RESULTS AND DISCUSSION

2.1 Friction Force and Wear Analysis

Fig. 2 shows the friction force curve of TCRB G01 toG07 with single/compound pits under starved lubrication. This study was about friction-induced vibration noise, so we think it is more direct here to use friction rather than friction coefficient. The friction force curve of G08 is provided as a reference.

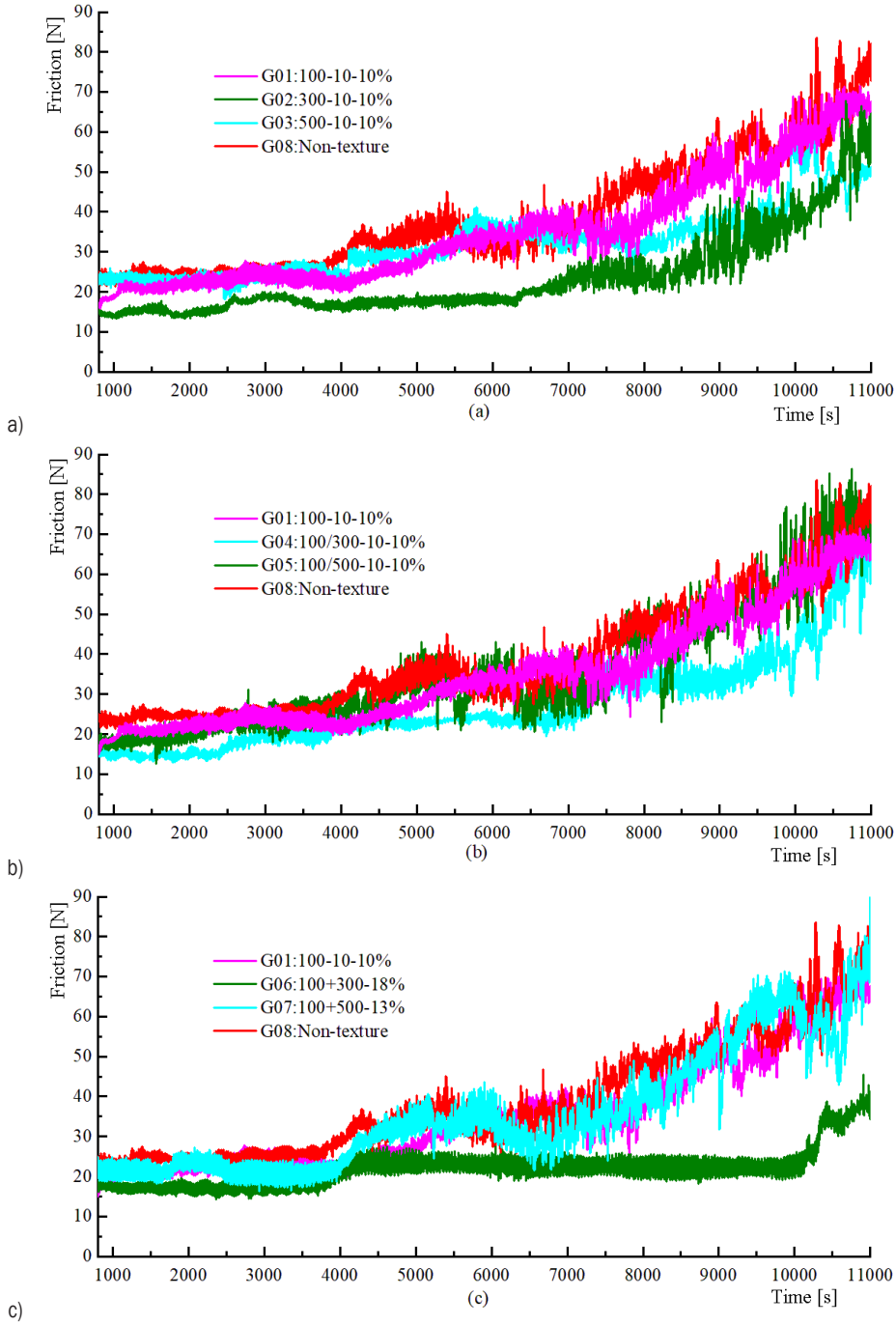

Fig. 2. Friction force curves of G01 to G08 under starved lubrication; a) friction force curves (G01, G02, G03 and G08), b) friction force curves (G01, G04, G05 and G08), and c) friction force curves (G01, G06, G07 and G08)

The label "G01:100-10-10%" stands for "Group number: diameter-depth-density".

From Fig. 2, the friction force of the TCRBs can be divided into three stages. Under starved lubrication conditions (initial 4000 s, approximately), the steady-state stage is characterised by pit storage of lubricating oil, uniform lubrication film on the contact surface, good contact mechanics, and a stable friction curve. The contact surface was partially crushed at the defect initiation and development stage (4000 s to 8000 s), and pits captured the worn nylon powder and debris. Nylon powder might come

from the wear of cylindrical roller and cage pocket hole, self-aligning thrust bearing, wear of cage and friction pair running-in process, etc. The debris might come from unpolished texture edges or texture edges crushed during the test. The lubricating oil in the pits played a secondary lubrication role, and the friction curve started to show an upward trend. In the failure-increasing stage (8000 s to 11000 s), the local crushing continued to deteriorate, the lubricating oil was gradually exhausted, and intermittent dry grinding occurred. The non-textured surface or pits could not store any more nylon powder and debris, and the wear was aggravated, leading to an accelerated increase in the friction curve. Taking Fig. 3c as an example, the friction curve of the texture bearing G06 was significantly lower than that of the smooth bearing G08, indicating that the texture can play a beneficial role in reducing friction and resisting wear.

Fig. 3 shows the wear loss on the shaft washer of each bearing group under starved lubrication conditions; the wear loss of the bearings containing single/compound pits was markedly reduced and lower than that of the non-textured surface bearing group. The wear loss for G02 was 3.38 mg, which was the lowest of all bearings tested. G03 and G06 reported a wear loss of 3.93 mg and 4.93 mg, respectively, at the medium level. The wear loss of G07 was 8.08 mg, which was identical to that of the non-textured G08, with a wear loss of 8.36 mg.

As shown in Fig. 3, an inflection point occurred when the pit diameter was 300 μm. The increase in the diameter of the pit indicates a reduction in the effective contact area, an increase in the contact stress (taking the texture bearing G02 and the non-textured smooth bearing G08 as examples, see Table 6), and an increase in the effective volume of the pit, serious collapse of the pit edge, and strong radial centrifugal movement of the nylon powder.

Fig. 4 shows the finite element analysis results of G02 and G08 thrust cylindrical roller bearings (1/18). In Fig. 4a, the nodes of G02 were 403280, the elements were 134702, and the maximum contact stress was 887.93 MPa. In Fig. 4b, the nodes of G08 were 412268, the elements were 97357, and the maximum contact stress was 722.83 MPa. The contact pressure value of finite element analysis was basically consistent with the theoretical calculation results in Table 6.

The worn surfaces of the shaft washers of G06 and G08 are shown in Fig. 5. From the wear marks and surfaces, in the compound textured bearing G06, the fatigue pitting was light, the debris on the contact surface was less and smaller, and the debris in the pit was larger. But in non-texture bearing G08, the fatigue

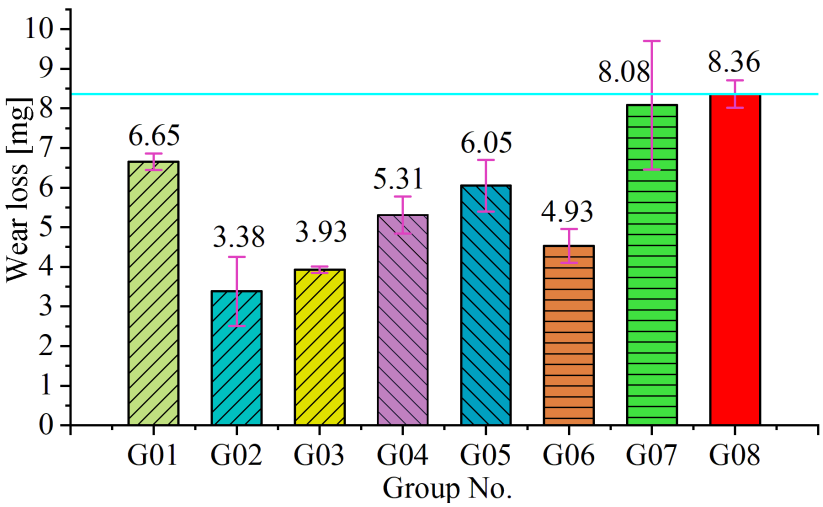

Fig. 3. *Wear losses of shaft washer of G01 to G08 under starved lubrication*

Table 6. *Contact pressure and contact area of single roller G02 and G08*

Group code	Load, Q [N]	Contact length, l [mm]	Elasticity modulus, E_1, E_2 [Pa]	Poisson's ratio μ_1, μ_2	Radius of roller, R_1 [mm]	Radius of contact surface of WS, R_2 [mm]	Contact half width, b [mm]	Contact pressure, [MPa]	Contact area, S [mm²]
G02	144.4	2.8	2.06E11	0.3	2.5	$+\infty$	0.038	864.66	0.213
G08	144.4	4	2.06E11	0.3	2.5	$+\infty$	0.032	718.75	0.256

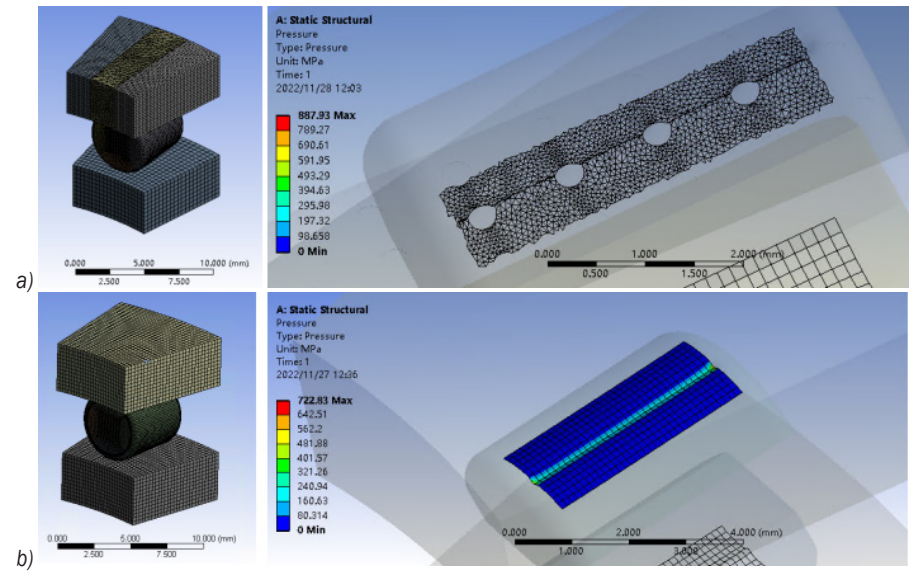

Fig. 4. *Finite element analysis (FEA) results of a) G02 and b) G08 thrust cylindrical roller bearings (1/18)*

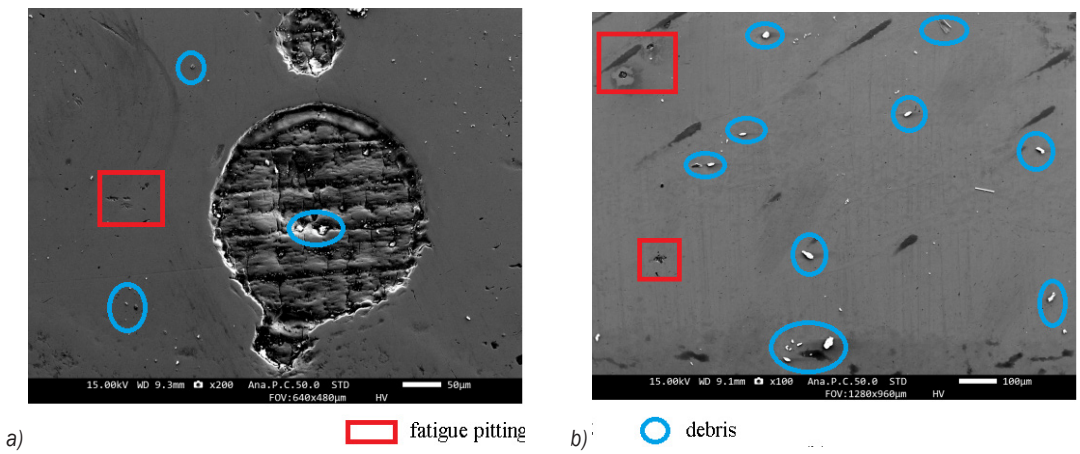

Fig. 5. *Worn surfaces of shaft washer of a) G06 and b) G08 under starved lubrication*

pitting was more serious and the debris was more and larger. Through comparative analysis, it can be seen that the pit texture can trap large debris and reduce the wear degree of the contact surface.

The effects of single/compound pits on the friction and wear performance of TCRBs were: (1) Compared to the non-textured TCRBs, the amount of debris left on the shaft washer of the single/compound pit texture was significantly reduced owing to the centrifugal throw effect during high-speed rotation [27]. This helped reduce the friction force and wear loss in the shaft washers in the TCRBs. (2) Single/compound pits reduced the effective contact area of the shaft washer [28]. The contact stress on the raceway was improved and the presence of surface pits reduced the contact area of the friction interface, thereby reducing the local contact stiffness. Simultaneously, the contact stress on the surface of the friction pair was distributed, improving the wear characteristics of the contact interface. (3) Laser surface texture technology improves fatigue and wear resistance and forms bionic anti-wear surfaces with "soft"–"hard" and "rigid"–"soft" phases. All bionic textured samples have positive effects on fatigue behavior through phase transformation and grain strengthening [29].

2.2 Effect of Single/Compound Pit Texture Surface on Friction-induced Vibration and Noise

The equivalent sound pressure level is defined as the sound pressure level averaged by the energy in a certain period of time. To evaluate the frictional

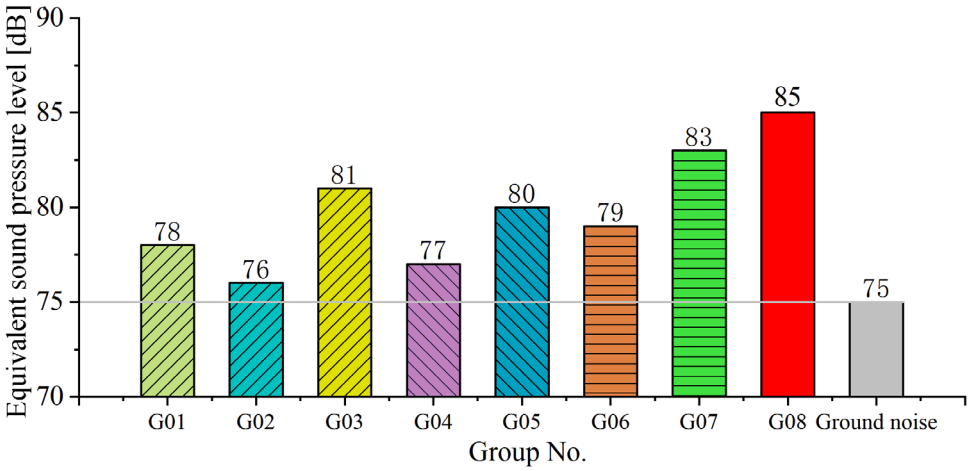

Fig. 6. *Equivalent sound pressure level of the non-textured surfaces and pit-textured surfaces*

noise level of the non-textured surface and single/compound pit-textured surface, an equivalent sound pressure level analysis was carried out on the noise sound pressure signals within 100 s in the stable stage, as shown in Fig. 6. The friction noise intensity of the non-textured bearing G08 was the highest at 85 dB, followed by single/compound pit-textured bearings G07, G03, and G05, at approximately 80 dB to -83 dB, all of which contained a texture with a pit diameter of 500 μm. In contrast, the intensity of the noise generated by the single-pit-textured bearing G02 was significantly lower (approximately 76 dB). This is similar to the background noise of 75 dB, indicating that approximately no noise was generated on the single pit-textured surface.

2.3 Time-frequency Analysis of Friction-induced Vibration and Noise

Time history records of the sound pressure signal and *Y*-direction acceleration were collected at approximately 3000 s. The pits can play a role in reducing vibration and noise [19], and [20].

Ming [30] studied a wavelet-spectrum autocorrelation method for rolling bearing composite-fault feature separation and concluded that under identical wavelet decomposition conditions, the wavelet-spectrum autocorrelation method was better than the wavelet-envelope spectrum feature separation. It had high engineering application value.

Wavelet transformation can select different time windows for different frequencies; a narrower time window for high-frequency signals and a wider time window for low-frequency signals. The wavelet transform of the known continuous signal $h(t)$ is defined as

$$W_{\varnothing}(a,\tau)=\frac{1}{\sqrt{|a|}}\int_{-\infty}^{+\infty}h(t)\varnothing^{*}\left[\frac{\tau-t}{a}\right]dt, \quad (2)$$

where a is the telescopic scale, τ is the shift factor, and $\varnothing(t)$ is a wavelet mother function, and it satisfies

$$C_{\varnothing}=\int_{-\infty}^{+\infty}\frac{\varnothing(\omega)}{\omega}d\omega<\infty, \quad C_{\varnothing}\neq 0. \quad (3)$$

The inverse transformation is defined as

$$h(t)=\frac{1}{C_{\varnothing}}\int_{-\infty}^{+\infty}\int_{0}^{+\infty}\frac{1}{a^{2}}W_{\varnothing}(a,\tau)\varnothing^{*}\left[\frac{\tau-t}{a}\right]dad\tau. \quad (4)$$

A time–frequency analysis of the noise and axial (*Y*) vibration acceleration was carried out to study the frequency variation of the test. As shown in Fig. 7, the change in the frictional contact caused by the roller element over the pit-textured surface did not change the dominant frequency of the sound pressure and vibration. However, significant energy distributions of G03, G07, and G08 were observed at a dominant frequency of 1500 Hz, causing significant screaming noise. The energies of G04 and G06 at the dominant frequency of 1500 Hz were insignificant. Therefore, there were no high-frequency screams during the entire process.

2.4˜ Frequency Spectrum Analysis of Friction-induced Vibration and Noise

The pit morphology and friction force of the contact surface are closely related to friction-induced vibration noise. To further investigate the influence of

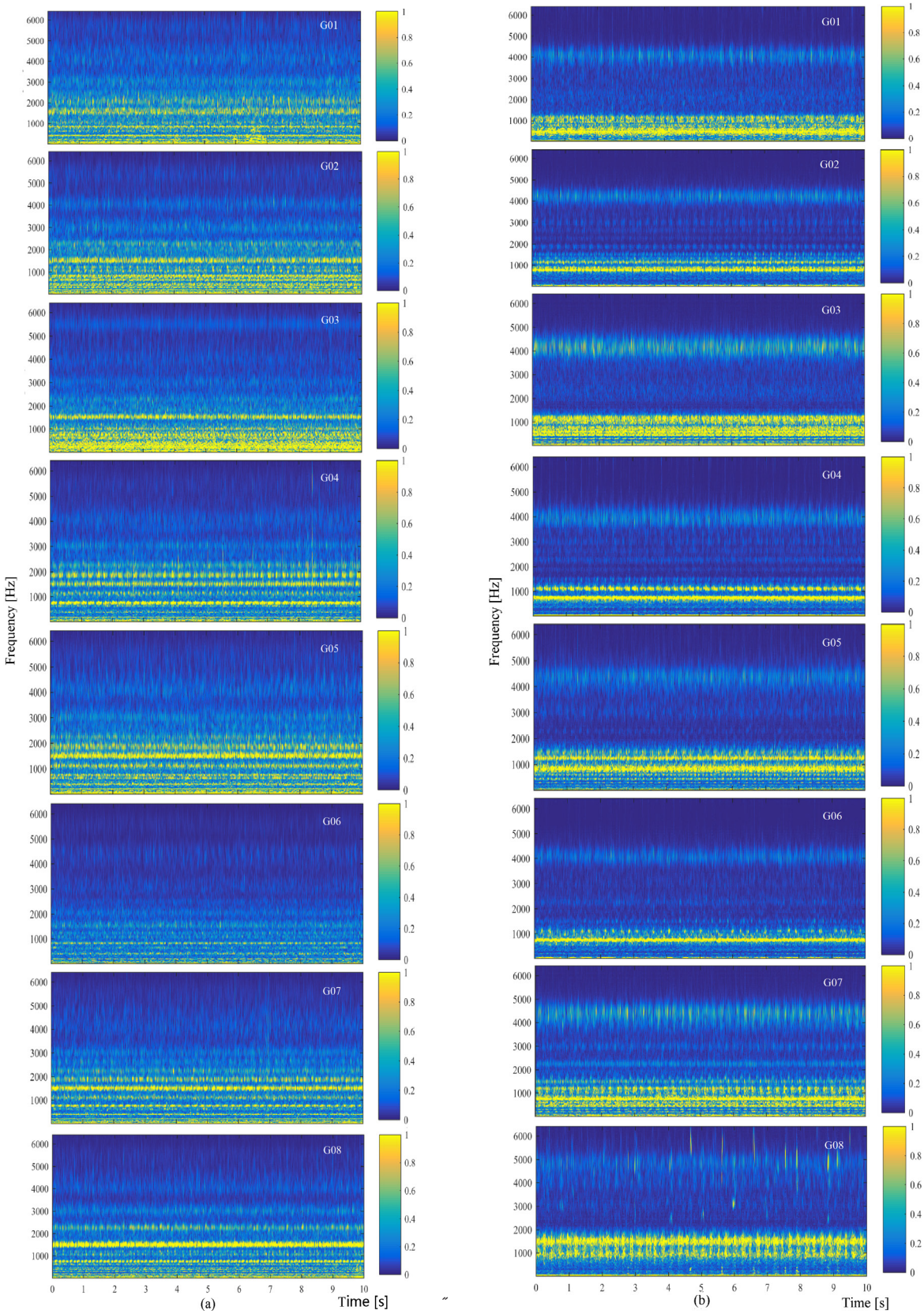

Fig. 7. *a) Time–frequency analysis of sound pressure, and b) vibration acceleration in friction (Y) direction*

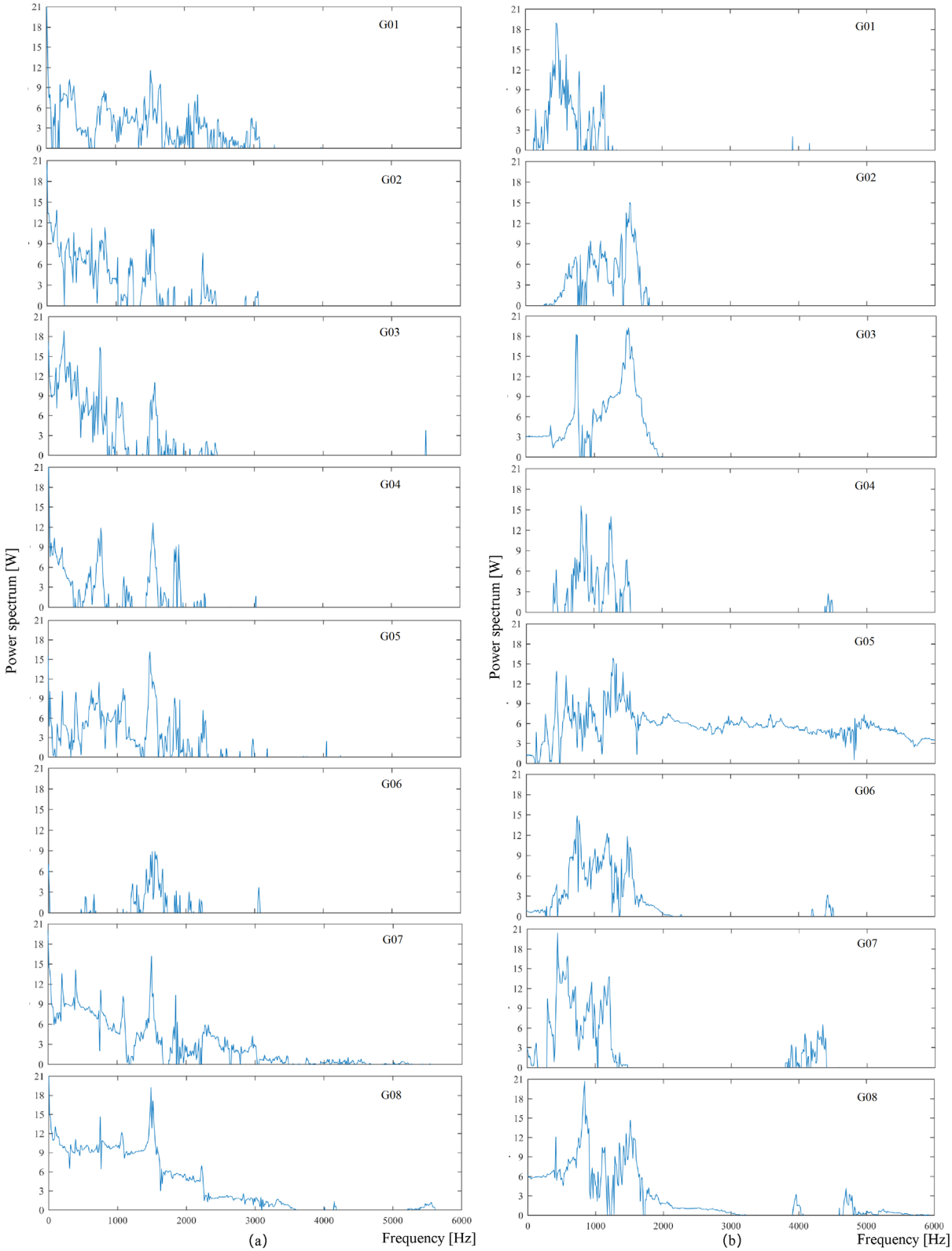

Fig. 8. *a) Power spectrum analysis diagram of noise pressure, and b) vibration acceleration in (Y) direction*

the single/compound pit-textured surface topography on vibration and noise, a frequency spectrum analysis of the friction-induced vibration noise signals and friction force was performed. The internal coherence of the signals is also discussed. Fig. 8 shows the power spectrum of noise pressure and vibration acceleration for non-textured surface bearings and different single/compound pit-textured bearings, reflecting the power distribution of these signals in the frequency domain (1500 Hz). The signal power of all pit-textured surface bearings was low at the primary frequency. G06 exhibited the lowest power spectrum at 1500 Hz.

2.5 Mechanism of Vibration and Noise Induced by Single/Compound Pit Texture Surface

The worn surface morphology of the single/compound pit-textured bearings consisted of macroscopic and microscopic pit morphologies. Macroscopic pits were composed of axial and radial spacing laws produced by laser marking equipment. The microscopic features include irregular features of the worn surfaces on the upper edges of the pits, such as wear debris layers, ploughing, and stripping. In this study, compared with the micro-irregular wear surface around the upper edge of the pits, the pits were the key reason for noise suppression.

The irregularity of the wear surface around the upper edge of the pit caused fluctuations in the friction force. It is often considered the actual excitation source of noise instability at the friction interface [31]. A pit-textured surface with specific geometries made it easier for wear debris to be trapped in pits and reduced noise tendencies. More importantly, pits can interrupt the continuous contact of the friction surface during rolling friction and reduce the effective contact area. Thus, they improve the surface-contact stress to suppress high-frequency friction fluctuations and interrupt the self-excited vibration of the friction system.

3 CONCLUSIONS

The effects of the single/compound pit texture on friction, wear performance, and friction-induced vibration noise characteristics of the TCRB were studied. The following conclusions were drawn.

1. Under starved lubrication, the friction force and wear loss on the single/compound pit-textured TCRBs were significantly lower than that on the non-textured surface bearings. The lowest wear loss was observed for G02. The friction force and wear loss were 39.6 % and 59.6 %, respectively, lower than the non-textured surface bearing.
2. Only 10mg of lubricating oil was added to each test, with the operation of the TCRB, the lubricating oil at the contact between the shaft washer surface and the rolling elements was gradually exhausted. The lubricating oil stored in the pits was continuously removed and the lubrication state of the system was maintained. The single/compound pits played a role in storing the lubricating oil and providing secondary lubrication to the bearing system.
3. The frequencies of the friction force, noise pressure signals, and vibration acceleration signals were approximately equal (1500 Hz) when there was significant noise. Friction force and vibration noise are closely related.
4. Noise and vibration were related to frictional fluctuations due to microscopic irregularities on wear surfaces, such as ploughing and abrasion debris layers. Single/compound pits texture contact surfaces with regular geometry made them easier to trap wear debris into the pits. Therefore, single and compound pits helped reduce irregularities and noise tendencies.

4 ACKNOWLEDGEMENTS

This work was supported by the National Key R&D Program of China (No. 2019YFB2004400) and the Chinese National Natural Science Foundation (No. U1708254). The authors sincerely thank the editors and reviewers for their efforts in improving this paper.

5 APPENDIX

The formula of contact pressure and contact area [32], since the thrust cylindrical roller bearing has 18 rollers, 1/18 of the bearing was taken for calculation. The meanings of the letters in the formula are shown in Table 4.

$$p_{\max} = \frac{2 \times Q}{\pi \times b \times l}, \tag{A1}$$

$$b = \sqrt{\frac{4}{\pi} \times \frac{1}{E^*} \times \frac{Q}{l} \times \frac{R_1 \times R_2}{R_1 + R_2}}, \tag{A2}$$

$$E^* = \frac{1-\mu_1^2}{E_1} + \frac{1-\mu_2^2}{E_2}, \tag{A3}$$

$$S = 2b \times l. \tag{A4}$$

5 REFERENCES

[1] Tala-ighil, N., Fillon, M. (2015). A numerical investigation of both thermal and texturing surface effects on the journal bearings static characteristics. *Tribology International*, vol. 90, p. 228-239, **DOI:10.1016/j.triboint.2015.02.032**.

[2] Wang, Q., Shi, F., Lee, S.C. (1997). A Mixed-TEHD model for journal-bearing conformal contact-Part II: Contact, film thickness, and performance analyses. *Journal of Tribology*, vol. 120, no. 2, p. 206-213, **DOI:10.1115/1.2834411**.

[3] Rosenkranz, A., Grützmacher, P.G., Murzyn, K., Mathieu, C., Mücklich, F. (2019). Multi-scale surface patterning to tune friction under mixed lubricated conditions. *Applied Nanoscience*, vol. 11, p. 751-762, **DOI:10.1007/s13204-019-01055-9**.

[4] Etsion, I. (2004). Improving tribological performance of mechanical components by laser surface texturing. *Tribology Letters*, vol. 17, p. 733-737, **DOI:10.1007/s11249-004-8081-1**.

[5] Mishra, S.P., Polycarpou, A.A. (2011). Tribological studies of unpolished laser surface textures under starved lubrication conditions for use in air-conditioning and refrigeration compressors. *Tribology International*, vol. 44, no. 12, p. 1890-1901, **DOI:10.1016/j.triboint.2011.08.005**.

[6] Olofinjana, B., Lorenzo-Martín, C., Ajayi, O.O., Ajayi, E.O. (2015). Effect of laser surface texturing (LST) on tribochemical films dynamics and friction and wear performance. *Wear*, vol. 332-333, p. 1225-1230, **DOI:10.1016/j.wear.2015.02.050**.

[7] Rodrigues, G.W., Bittencourt, M.L. (2020). Surface virtual texturing of the journal bearings of a three-cylinder ethanol engine. *Industrial Lubrication and Tribology*, vol. 72 no. 9, p. 1059-1073, **DOI:10.1108/ilt-09-2019-0380**.

[8] Marian, M., Grützmacher, P.G., Rosenkranz, A., Tremmel, S., Mücklich, F., Wartzack, S. (2019). Designing surface textures for EHL point-contacts - Transient 3D simulations, meta-modeling and experimental validation. *Tribology International*, vol. 137, p. 152-163, **DOI:10.1016/j.triboint.2019.03.052**.

[9] Marian, M., Almqvist, A., Rosenkranz, A, Fillon, M. (2022). Numerical micro-texture optimization for lubricated contacts-A critical discussion. *Friction*, vol. 10, p. 1772-1809, **DOI:10.1007/s40544-022-0609-6**.

[10] Costa, H.L., Schille, J., Rosenkranz, A. (2022). Tailored surface textures to increase friction-A review. *Friction*, vol. 10, p. 1285-1304, **DOI:10.1007/s40544-021-0589-y**.

[11] König, F., Rosenkranz, A., Grützmacher, P.G., Mücklich, F., Jacobs, G. (2020). Effect of single- and multi-scale surface patterns on the frictional performance of journal bearings - A numerical study. *Tribology International*, vol. 143, art. ID. 106041, **DOI:10.1016/j.triboint.2019.106041**.

[12] Grützmacher, P.G., Rosenkranz, A., Szurdak, A., König, F., Jacobs, G., Hirt, G., Mücklich, F. (2018). From lab to application - Improved frictional performance of journal bearings induced by single- and multi-scale surface patterns. *Tribology International*, vol. 127, p. 500-508, **DOI:10.1016/j.triboint.2018.06.036**.

[13] Segu, D.Z., Lu, C., Hwang, P., Kang, S. (2021). Optimization of tribological characteristics of a combined pattern textured surface using Taguchi design. *Journal of Materials Engineering and Performance*, vol. 30, p. 3786-3794, **DOI:10.1007/s11665-021-05673-9**.

[14] Segu, D.Z., Hwang, P. (2015). Friction control by multi-shape textured surface under pin-on-disc test. *Tribology International*, vol. 91, p. 111-117, **DOI:10.1016/j.triboint.2015.06.028**.

[15] Segu, D.Z., Hwang, P. (2016). Effectiveness of multi-shape laser surface texturing in the reduction of friction under lubrication regime. *Industrial Lubrication and Tribology*, vol. 68, p. 116-124, **DOI:10.1108/ILT-03-2015-0041**.

[16] Kim, J., Choi, S., Segu, D.Z., Jung, Y., Kim, S.S. (2014). Improvement of tribological characteristics of multi-scale laser-textured surface in terms of lubrication regime. *Tribology and Lubricants*, vol. 30, no. 1, p. 59-63, **DOI:10.9725/kstle.2014.30.1.59**.

[17] Milčić, D., Alsammarraie, A., Madić, M., Krstić, V., & Milčić, M. (2021). Predictions of Friction Coefficient in Hydrodynamic Journal Bearing Using Artificial Neural Networks. *Strojniški vestnik - Journal of Mechanical Engineering*, vol. 67, no. 9, p. 411-420, **DOI:10.5545/sv-jme.2021.7230**.

[18] Wrzochal, M., Adamczak, S., Domagalski, R., Piotrowicz, G., & Wnuk, S. (2022). New device proposed for industrial measurement of rolling bearing friction torque. *Strojniški vestnik - Journal of Mechanical Engineering*, vol. 68, no. 10, p. 610-622, **DOI:10.5545/sv-jme.2022.275**.

[19] Sudeep, U., Pandey, R.K., Tandon, N. (2013). Effects of surface texturing on friction and vibration behaviors of sliding lubricated concentrated point contacts under linear reciprocating motion. *Tribology International*, vol. 62, p. 198-207, **DOI:10.1016/j.triboint.2013.02.023**.

[20] Sudeep, U., Tandon, N., Pandey, R.K. (2016). Vibration studies of lubricated textured point contacts of bearing steels due to surface topographies: Simulations and experiments. *Tribology International*, vol. 102, p. 265-274, **DOI:10.1016/j.triboint.2016.05.040**.

[21] Gupta, N., Tandon, N., Pandey, R.K., Vidyasagar, K.E., Kalyanasundaram, D. (2020). Tribological and vibration studies of textured spur gear pairs under fully flooded and starved lubrication conditions. *Tribology Transactions*, vol. 63, p. 1103-1120, **DOI:10.1080/10402004.2020.1794093**.

[22] Hu, L., Mo, J., Wang, D., Yang, J., Chen, G., Zhu, M. (2016). Groove-textured and pit-textured surfaces to suppress friction-induced squeal noise. *China Mechanical Engineering*, vol. 27, no. 9, p. 1158-1164, **DOI:10.3969/j.issn.1004-132X.2016.09.004**. (in Chinese)

[23] Wrzochal, M., Adamczak, S., Piotrowicz, G., & Wnuk, S. (2022). Industrial experimental research as a contribution to the development of an experimental model of rolling bearing vibrations. *Strojniški vestnik - Journal of Mechanical Engineering*, vol. 68, no. 9, p. 552-559, **DOI:10.5545/sv-jme.2022.184**.

[24] Chernets, M., Opielak, M., Kornienko, A., & Radko, O. (2021). Predictive Estimation of Sliding Bearing Load-Carrying Capacity and Tribological Durability. *Strojniški vestnik - Journal of Mechanical Engineering*, vol. 67, no. 7-8, p. 363-368, **DOI:10.5545/sv-jme.2021.7139**.

[25] Kydyrbekuly, A., Ibrayev, G., Ospan, T., & Nikonov, A. (2021). Multi-parametric Dynamic Analysis of a Rolling Bearings

System. *Strojniški vestnik - Journal of Mechanical Engineering*, vol. 67, no. 9, p. 421-432, **DOI:10.5545/sv-jme.2021.7178**.

[26] Long, R., Ma, Q., Jin, Z., Zhang, Y., Han, H., Sun, S., Du, X. (2022). Tribological behavior of dimples textured rolling element bearings under stepped load and starved lubrication. *Industrial Lubrication and Tribology*, vol. 74, no. 7, p. 876-883, **DOI:10.1108/ilt-04-2022-0150**.

[27] Grützmacher, P.G., Rosenkranz, A., Rammacher, S., Gachot, C., Mücklich, F. (2017). The influence of centrifugal forces on friction and wear in rotational sliding. *Tribology International*, vol. 116, p. 256-263, **DOI:10.1016/j.triboint.2017.07.021**.

[28] Rosenkranz, A., Grützmacher, P.G., Gachot, C., Costa, H.L. (2019). Surface texturing in machine elements − a critical discussion for rolling and sliding contacts. *Advanced Engineering Materials*, vol. 21, no. 8, art. ID 1900194, **DOI:10.1002/adem.201900194**.

[29] Li, H., Zhou, H., Zhang, D.P., Zhang, P., Zhou, T. (2022). Influence of varying distribution distance and angle on fatigue wear resistance of 40Cr alloy steel with laser bionic texture. *Materials Chemistry and Physics*, vol. 277, art. ID 125515, **DOI:10.1016/j.matchemphys.2021.125515**.

[30] Ming, A. (2013). Compound fault features separation of rolling element bearing based on the wavelet decomposition and spectrum auto-correlation. *Journal of Mechanical Engineering*, vol. 49, no. 3, p. 80-87, **DOI:10.3901/jme.2013.03.080**.

[31] Mo, J., Wang, Z., Guangxiong, C., Shao, T., Zhu, M., Zhou, Z.R. (2013). The effect of groove-textured surface on friction and wear and friction-induced vibration and noise. *Wear*, vol. 301, no. 1-2, p. 671-681, **DOI:10.1016/j.wear.2013.01.082**.

[32] Popov, V.L. (2010). *Contact Mechanics and Friction: Physical Principles and Applications*. Springer, Springer Heidelberg **DOI:10.1007/978-3-642-10803-7**.